

1 **Paper-based Sensing of Fucosylated Biological Compounds**

2 Fatima Enam¹, Emily Kramer¹, Frederick Robinson², Andrea Alvarez-Acosta¹, Rebecca
3 Cademartiri³, Thomas J. Mansell*¹

4 1. Department of Chemical and Biological Engineering, Iowa State University, Ames, IA, 50011

5 2. Department of Bioengineering, Rice University, Houston, TX, 77005

6 3. Department of Material Science and Engineering, Iowa State University, Ames, IA, 50011

7 *Correspondence: mansell@iastate.edu

8

9 **Summary**

10 Advances in sensing technology have enabled rapid analysis of various biomolecules including
11 complex carbohydrates. However, glycan analysis is limited by the throughput and complexity of
12 assays for quantifying them. We describe a simple, low-cost enzymatic assay for the rapid
13 analysis of fucosylation, down to linkage specificity, and its application to high-throughput
14 screening of biologically relevant fucosylated compounds, to facilitate simple and
15 straightforward analytical techniques. Paper-based devices integrate biosensor platforms and
16 other diagnostic assays by fusing them with wax printing technology, making their fabrication
17 even more inexpensive and simple. The specificity of the assay is established by linkage-
18 specific glycosidic enzymes and the colorimetric output is visible to the naked eye, with costs
19 that are lower than fluorescence/luminescence-based assays (\$0.02/reaction). This platform
20 was further improved by enhancing storage stability to retain analytical performance over time
21 using desiccation and freeze-drying techniques. The assay platform allows analysis of hundreds
22 of samples in minutes and we anticipate that this rapid and simple analytical method will be
23 extended towards developing a universal glyco-barcoding platform for high throughput
24 screening of glycosylation.

25

26 **Keywords:** Fucose; paper-based device; high throughput sensing; human milk

27 oligosaccharides

28 **Introduction**

29 L-fucose is a common terminal sugar in glycans and oligosaccharides that has been attributed
30 to several key metabolic and structural functions^{1,2}. It is found as a terminal modification on N-,
31 O- or lipid-linked oligosaccharides and as a core modification on N-glycans or linked to serine
32 (Ser) or threonine (Thr) on proteins. It is also the second most abundant terminal
33 monosaccharide moiety, after sialic acid³, found in mammalian carbohydrates to form various
34 recognition motifs on many glycoproteins and glycolipids. Most notably, fucose has important
35 roles as a component of ABO blood group antigens⁴, a key modulator of interactions in the
36 immune system and in human breast milk.

37 Breastfeeding is associated with a lower risk of infection in babies and the underlying
38 mechanism has been linked to the diverse range of complex sugars^{5,6}, the human milk
39 oligosaccharides (HMOs)⁷. A large majority of these HMOs are fucosylated^{8,9}, with 2'-
40 fucosyllactose (2'-FL) being the most abundant HMO comprising approximately 2 g/L. Notably,
41 fucosylated HMOs inhibit binding and colonization of pathogens^{10,11} and provide protection
42 against diarrhea associated with stable toxin of *Escherichia coli*^{12,13}. Supplementation of 2'-FL to
43 infant diet showed improved outcomes on innate and adaptive immune profiles¹⁴, and
44 increasing evidence of its health benefits has led to its commercialization as a supplement in
45 infant formula.

46 Similarly, the lipopolysaccharide (LPS) of *Helicobacter pylori* strains expresses Lewis
47 antigens (Le^x, Le^y, H type I blood group structures) resembling the surface of host gastric
48 epithelial cells¹⁵ and upon *H. pylori* infection, this may cause antibodies to bind not only to the
49 bacteria but also the host epithelium resulting in tissue destruction. This antigen mimicry, being
50 analogous to ABO blood group antigens, may also provide persistence through immune

51 evasion¹⁶. Fucosylation is also an important oligosaccharide modification involved in cancer and
52 inflammation¹⁷. The majority of human immunoglobulins (IgG) contain core fucosylation of the
53 N-glycan in the Fc region, the absence of which has shown to have enhanced antibody-
54 dependent cellular cytotoxicity (ADCC) activity due to increased binding affinity^{18,19}.

55 Despite the biological importance of fucose, a critical obstacle in elucidating its
56 biochemical roles lies in the technical difficulties associated with detection and analysis,
57 especially with determining carbohydrate linkage positions. Current state-of-the-art methods for
58 determining fucosylation include capillary electrophoresis (CE), mass spectrometry (MS),
59 HPAEC-PAD²⁰, NMR²¹ or glycan sequencing, which are laborious methods requiring
60 specialized equipment and sample preparation. Another established method with higher
61 throughput is the spectrophotometric detection of free L-fucose following defucosylation by
62 measuring the formation of NADH²². Seydametova et al. demonstrated quantitative assays for
63 2'-FL, utilizing hydrolysis by fucosidases^{23,24}. Their efforts, however, focused on a single
64 biological molecule and by spectrophotometrically measuring the end-point nicotinamide
65 adenine dinucleotide phosphate (NADP⁺) formed after an hour. Advances in synthetic biology
66 have enabled high-throughput screening via biological components that have been
67 standardized, for example, whole cell biosensors allow for the transduction of analyte
68 concentrations to changes in gene expression that facilitate high-throughput assaying²⁵⁻²⁷. We
69 previously demonstrated a genetically encoded whole cell biosensor to facilitate metabolic
70 engineering by enabling the linkage-specific high-throughput detection of 2'-FL and four other
71 HMOs²⁸. The study demonstrated orthogonal screening of HMO structures, but entails culturing
72 bacterial strains relatively expensive equipment to read fluorescence, e.g., flow cytometer or
73 microplate reader.

74 To leverage the specificity and sensitivity of this assay to a faster and cheaper format,
75 we sought to transfer the underlying detection mechanism to a paper-based assay. Paper
76 based devices can be preferable to whole-cell assays, especially at the point of care, owing to

77 their simplicity, low-cost and portability and the minimal resources, time and equipment required
78 in their fabrication²⁹. These devices also allow for rapid analysis of multiple samples in parallel.
79 Colorimetric assays producing a visual readout are a common choice for paper-based
80 devices^{30–32}, with their usefulness lying in the formation of brightly colored formazan products
81 upon reduction. Notably, they can be particularly useful in point-of-use or low-resource settings.

82 Here, we demonstrate a standard colorimetric assay for a simple, rapid, low-cost
83 linkage-specific sensing system for fucosylated biomolecules (**Figure 1A**). To create this device,
84 we expressed enzymes specific for three of the most common fucose linkages heterologously in
85 *E. coli* and immobilized them on to the paper device. Using a formazan reduction assay coupled
86 with fucose dehydrogenase, we then assay for the release of free L-fucose. The assay has a
87 limit of detection of below 20 mg/L for 2'-FL and can detect fucose linked to several types of
88 biomolecules, including HMOs, Lewis structures, and N-glycans. Finally, the assay can detect
89 fucosylated compounds in complex body fluid matrices such as human milk and simulated
90 urine.

91 **Results**

92 **Fucosidases act as linkage-specific detection elements for fucosylated HMOs**

93 To couple reduction of colorimetric dye to the quantification of 2'-FL, we used fucosidases
94 known in literature^{33,34} to be specific to the carbohydrate linkage to fucosylated molecules. Free
95 fucose can then be assayed using a redox-coupled reaction in which fucose dehydrogenase
96 (FDH) oxidizes L-fucose to fuconolactone, creating NADPH, which reduces the formazan dye.
97 To confirm that this coupled reaction scheme would produce NADPH, we incubated 2'-FL (Fuc-
98 α -1,2-Gal- β -1,4-Glc) with commercial purified α -1,2-fucosidase to cleave the fucose and in the
99 presence of commercial FDH and NADP⁺. By following the increase in absorbance at 340 nm
100 due to reduction of NADP⁺ on a microplate reader, we verified the redox reaction undergone by
101 the cleaved fucose (**Supplementary Figure S1A**).

102 However, the use of two purified enzymes can be expensive. To achieve an efficient,
103 low-cost detection system, we hypothesized that using a bacterial host as a heterologous
104 system for the production of high levels of functionally active recombinant enzymes would be
105 cost-effective. Because it efficiently and orthogonally cleaved L-fucose from 2'-FL in the context
106 of a whole-cell biosensor³⁵ we chose to express the soluble glycosyl hydrolase domain of AfcA,
107 an α -1,2-fucosidase from *Bifidobacterium bifidum*³⁶ under a constitutive promoter, to liberate
108 fucose from 2'-FL³⁵. Cell lysate from overnight cultures of *E. coli* BL21 (DE3) expressing AfcA
109 was added to purified FDH with NADP⁺ as before. We detected reduction to NADPH when 2'-FL
110 was added as an analyte but not on the isomeric HMO 3-FL (Gal β -1,4(Fuc- α -3)Glc)
111 (**Supplementary Figure S1A**). No background redox activity associated with the components in
112 the cell lysate itself was observed in an empty vector control over a period of one hour. This
113 strain served as a control in subsequent experiments, where the background noise from the
114 crude cell lysate was noted for all measurements.

115

116 **Tetrazolium dye allows colorimetric detection of fucosylated compounds**

117 Once we confirmed that the sequential reactions of cleavage by fucosidase followed by
118 oxidation by fucose dehydrogenase generated the reducing co-factor, we added a redox-
119 sensitive dye to make the assay visible by the naked eye. Tetrazolium salts have been
120 historically used for testing cell viability, proliferation and cytotoxicity^{37,38}. We chose 2-(4-
121 iodophenyl)-3-(4-nitrophenyl)-5-phenyl-2H-tetrazolium chloride (INT), which in the presence of
122 the intermediate electron carrier, 5-methyl-phenazine methyl sulfate (PMS), is reduced to an
123 insoluble formazan. This precipitate absorbs light at a wavelength of 500 nm and provides a
124 robust signal visible to the naked eye³⁹. The generated NADPH, when coupled to INT, forms a
125 stable red formazan (**Figure 1B**) and, being stoichiometrically proportional to the fucose
126 concentration allows us to directly quantify the fucose. We determined the optimum pH and

127 buffer conditions for the enzyme cocktail in the assay and coupled it with the INT/PMS assay to
128 establish a colorimetric assay protocol.

129 We first sought to quantify free fucose with FDH from cell lysate. An intense color change was
130 observed with 500 mg/L L-fucose resulting in a 100% increase in absorbance within a few
131 seconds as read on a plate reader at 500 nm (**Figure 1C**). The reaction contains 2.5 μg of L-
132 fucose with NADP^+ present in excess. In contrast, by measuring the NADPH formation by
133 reading the absorbance at 340 nm, a 30% increase in absorbance was seen at equivalent L-
134 fucose concentrations, which is to be expected since the molar extinction coefficient of INT
135 formazan is $18000 \text{ M}^{-1}\text{cm}^{-1}$ compared to $6220 \text{ M}^{-1}\text{cm}^{-1}$ for NADPH. Thus, the colorimetric
136 system showed greater sensitivity than changes in NADPH readout as demonstrated by the
137 slopes in **Supplementary Figure S3A**. Notably, minimal background was again observed with
138 the empty vector control. In addition, the switch to a colorimetric reaction allowed us to scale
139 down the reaction volume to 20 μL .

140 To demonstrate the utility of the assay in reliably detecting fucosylated molecules, we used the
141 assay to detect 2'-FL using additional crude cell lysate from cells expressing pAfcA. We titrated
142 the amount of cell lysate needed for optimum signal. For each 20 μL reaction, 5 μL lysate was
143 added. This also exhibited strong absorbance, a four-fold increase, with 2'-FL (300 mg/L) at the
144 same concentration of L-fucose (300 mg/L), containing, as previously tested (**Figure 1D**). The
145 linkage specificity was validated by the lack of significant increase in absorbance when tested
146 with its isomer 3-FL, indicating that the α -1,3 linkage was not defucosylated. Similarly, we went
147 on to demonstrate that this method can be extended to the detection of α -1,3 linked fucose as
148 well by using lysate of cells harboring plasmid pAfcB expressing α -1,3-fucosidase under
149 identical experimental conditions. We observed a 1.4-fold change in absorbance with 3-FL but
150 no color change was observed with 2'-FL (**Supplementary Figure S1B**). Similar to our previous
151 biosensors, this assay also demonstrated linkage specificity and the ability to distinguish
152 between isomeric HMOs.

153

154 **Fabrication of paper-based platform**

155 Once the colorimetric assay was developed, we focused on translating it to a paper-based
156 assay. Paper-based devices are fabricated from cellulose because it has advantages of being
157 low-cost, abundant, lightweight, biodegradable and biologically compatible^{40,41}. In addition, its
158 porosity and hydrophilicity offers wicking properties due to capillary action that can handle small
159 volumes of liquid with no external pumping⁴². To create our device, we used Whatman Grade 3
160 chromatography paper and defined the hydrophilic area using wax-printing method owing to its
161 ease of printing using commercially available printers. The design layout for the paper
162 corresponded to the dimensions of a standard 96-well plate⁴³. We chose this to accommodate
163 distinct test zones for independent reactions that can be carried out in parallel, also allowing for
164 the use of multi-channel pipettors for rapid assaying. Once printed, we melted the wax in an
165 oven. To ensure fully formed barriers, we observed the bottom side of the paper. Prior to
166 heating, no pattern is visible at the back. Upon heating, the wax melts and vertically penetrates
167 through the porous fiber network⁴⁴, which becomes visible on the bottom. This allows for the
168 aqueous sample and reagents to be contained within spatially separated hydrophilic zones.
169 There is also some lateral diffusion of the ink which reduces the diameter of the detection zone,
170 but this was taken into account during the design to ensure appropriate dimensions. We
171 designed the template with each well having a line thickness of 1 mm and internal diameter of 5
172 mm; after heating, the diameter was reduced to 4 mm. Once cooled, we further tested the
173 hydrophobic barriers for leaks by addition of colored water and looking for any sort of bleeding
174 outside of the well. If the liquid failed to contain, the paper was heated longer until no bleed-
175 through was visible. The procedure is illustrated in **Figure 2** and detailed in the Methods. Once
176 the device was ready to use, the enzymes were directly applied to the detection zones. A
177 master mix containing NADP⁺ dissolved in Tris-HCl buffer (pH 9.5) was then added to wet the
178 test zones, followed by the analyte to be tested. Immediately following that, the dye was applied

179 and allowed to dry under ambient conditions before scanning and analysis (**Supplementary**
180 **Figure S2**). In our experiments, it took less than 1 min from the addition of the dye for a
181 detectable color change in the test zones to occur (**Supplementary Video S1**).

182

183 **Paper-based sensing for distinguishing fucosylated HMOs**

184 Next, we implemented this paper-based colorimetric assay for distinguishing three fucosylated
185 HMOs: 2'-FL (Fuc- α -1,2-Gal- β -1,4-Glc), 3-FL (Gal- β -1,4(Fuc- α -3)Glc) and DFL (Fuc- α -1,2-Gal- β -
186 1,4(Fuc- α -3)Glc). We also tested for GDP-L-fucose, the donor substrate, a key component in
187 the biosynthesis of fucosylated HMOs^{45,46}. Either synthetic routes for 2'-FL and 3-FL,
188 enzymatic⁴⁷ or microbial via metabolic engineering⁴⁵, take place via GDP-L-fucose which can be
189 present in the final product at different levels. It is imperative that our assay is not sensitive to
190 GDP-L-fucose for its use in analysis of carbohydrate production from microbial sources. For the
191 assay we spotted the required enzymes on to the paper: either no enzyme as control and for
192 background reduction, only FDH for L-fucose and GDP-fucose detection, FDH and AfcA for 2'-
193 FL detection, FDH and AfcB for 3-FL detection and combination of FDH, AfcA and AfcB for DFL
194 detection. This was followed by the NADP⁺ dissolved in the buffer, the respective analytes and
195 the dye. The paper was allowed to dry and for the color to fully develop for an hour at room
196 temperature before analysis. We first tested if the two isomers, 2'-FL and 3-FL were
197 distinguishable and if there was any crosstalk. We had established earlier the lack of substrate
198 promiscuity in AfcA and AfcB in the context of the whole cell biosensor²⁸. No fucose was
199 liberated from 3-FL when AfcA was present (**Figure 3A**). **Figure 3B** shows a 25-reaction array
200 to distinguish three fucosylated HMOs. The control zones (top row with no added enzymes and
201 left column with no added substrate) showed no color change and the values obtained were
202 noted to account for the background signal from the dye and improve the accuracy of the assay.
203 Notably, no residual activity was observed with the concentrations of cell lysate used. An
204 intense color change from yellow to red was observed with free L-fucose when FDH was

205 present, as expected. This served as a positive control, confirming the activity of the FDH. With
206 2'-FL, a color change was observed only when AfcA was present to cleave the α -1,2-linked
207 fucose. We thus obtained a signal only when AfcA or both AfcA and AfcB were present. We
208 obtained similar results with 3-FL when AfcB was present. We did not observe any color change
209 with GDP-fucose implying the lack of enzymatic activity of FDH on GDP-fucose as a substrate
210 (data not shown).

211 We generated the respective calibration curves by the addition of a series of dilutions of
212 2'-FL and 3-FL in range 0-6000 mg/L. We then scanned the paper device using a desktop
213 scanner and analyzed the digital image on the green intensity channel. We quantified the color
214 change in the test zones, and converted the color change value into the corresponding
215 concentrations using the calibration curve for the assay (**Figure 3C, 3D**). The experimental data
216 were fitted into a 4-parameter logistic model (4PL) using MATLAB and the resulting transfer
217 functions revealed the dynamic range and limits of detection. The calibration curve for 2'-FL
218 showed a wide dynamic range between 150 and 2500 mg/L of 2'-FL (0.3-5 mM) and the limit of
219 detection (LoD) was found to be below 20 mg/L (0.04 mM) which satisfies the levels at which
220 these biological molecules are produced either naturally or via synthesis. For example,
221 Baumgärtner *et al.* engineered an *E. coli* strain to produce 2'-FL at levels of up to 21 g/L⁴⁵ and
222 analysis of HMOs in human milk shows 2'-FL to be present 60-15000 mg/L^{48,49}, which is well
223 within the limit of our device. Although the limit of detection is five-fold higher than our whole-cell
224 biosensor, the dynamic range for this device is much wider. Similarly, we characterized the
225 assay for 3-FL (**Figure 3D**) and the dynamic range of detection was found to be between 250
226 and 900 mg/L and the limit of detection below 250 mg/L (0.5 mM).

227 We also measured the absorbance values of the series of 2'-FL concentrations in a 96-
228 well paper plate on a microplate reader to see the correlation with the values obtained from the
229 paper-based assay. **Supplementary Figure S3B** shows the direct correlation of the

230 absorbance values as measured with a plate reader with the values from the paper-based
231 assay which correlate quite well.

232

233 **Stability of paper-based sensor**

234 Since the intrinsic instability of enzymes or proteins in general, makes it challenging for them to
235 be used for downstream applications, it was important to establish that our assay was functional
236 over a longer period of time. Different strategies have been developed to produce more stable
237 proteins and improve storage stability and shelf-life. The most frequently used method,
238 especially in the biopharmaceutical industry is drying^{50,51}. We spotted the enzymes on the test
239 zones and either dried it at room temperature or by lyophilization. We then evaluated the
240 stability of the enzymes on the cellulose matrix by storage at room temperature or at 4 °C. We
241 performed the assay for 2'-FL detection under the four different conditions over a period of 45
242 days and imaged the wells to confirm expression of the enzymes (**Supplementary Figure**
243 **S3C**). The desiccated enzymes maintained the similar activity over a period of one week, and
244 slowly started to decline. In 5 weeks, the activity dropped to 50% of the original, under both
245 storage conditions, and to 35% in 45 days. However, when lyophilized, 70% of its activity was
246 retained after 45 days. It was noticed that with refrigeration, the decline in activity was slower
247 compared to storage at room temperature. In solution, the enzyme master mix loses its activity
248 at room temperature in one day and in less than a week at 4 °C. Overall, the data demonstrates
249 sufficient stability of the paper-based sensor, especially under lyophilization. The assay can be
250 stored at room temperature for shorter durations, avoiding the need for cold-chain. Beyond
251 portability, immobilization of the enzymes enables minimal sample handling and cost and easy
252 operation, without the need for specialized equipment and skills.

253

254 **Analysis of fucosylated HMOs in breast milk and maternal/infant urine**

255 There is good evidence showing positive roles played by HMOs in breast milk, especially
256 fucosylated HMOs, on infant health. The α -1,2 fucosyltransferase (FUT2) gene catalyzes the
257 transfer of α -1,2-linked fucose residue, while the α -1,3/4 fucosyltransferase (FUT3) transfers α -
258 1,3-linked fucose residues to HMOs. Secretor status (harboring a functional copy of the FUT2
259 gene) can be established by profiling of HMOs in breast milk⁵². This variation in the composition
260 of HMOs in different mothers can provide some infants advantages over others. We tested if our
261 assay was capable of detecting and quantifying 2'-FL and 3-FL in human breast milk to help
262 identify secretors. As a control, we used powdered cow's milk, reconstituted to mimic breast
263 milk. We also chose to validate the quantitation using HPLC/MS-MS based on standard
264 retention times and mass spectrometric analysis. For the human breast milk samples, we
265 observed a color change indicating a concentration of 5,012 mg/L of 2'-FL (**Figure 4A**), which
266 we confirmed with a series of dilutions, and consistent with the 5-15 g/L of HMO typically
267 observed⁴⁹. The signal from the paper-based assay indicating higher 2'-FL concentrations may
268 be attributed to the presence of other α -1,2-fucosylated HMOs, such as lacto-N-fucopentaoses
269 (LNFP I, II, III and V). The concentration of 3-FL was below the detection limit of the paper-
270 based assay. However, we observed a color change once the samples were concentrated five
271 and ten-fold (**Figure 4B**). 3-FL was found at 138 mg/L which corresponds to values found in
272 literature⁴⁹. We observed no color change with the cow's milk samples, validating the
273 robustness of the assay in measuring fucosylation in biological fluids. To validate the assay,
274 characterization of isomers, 2'-FL and 3-FL, were carried out using mass spectrometry.
275 Although we were able to get adequate separation between the 2'-FL and 3-FL peaks, there
276 was overlap. The peaks were fully resolved by utilizing differences in m/z ratios of the
277 deprotonated negative ions (MS) in conjunction with the difference in retention time (HPLC) to
278 resolve the isomers (**Supplementary Figure S4**). To confirm the identity of the peaks, we also
279 carried out an exoglycosidase (α -1,2-fucosidase or α -1,3-fucosidase) digest. Treatment with
280 either α -1,2-fucosidase or α -1,3-fucosidase resulted in removal or major reduction of the

281 expected peaks (**Supplementary Figure S5**). HMOs have also been detected in the serum and
282 urine of mothers, with 2'-FL at the highest concentrations in secretors (20 mg/L)⁵³. Studies have
283 also shown high resemblance of HMO profiles in infant urine to mother's breast milk, as some
284 are absorbed and reach the systemic circulation and excreted in urine⁵⁴. These samples can
285 serve as excellent indicators of availability of fucosylated HMOs to infants, allowing for
286 supplementation when needed. We spiked non-biological urine containing constituents that
287 mimic human urine with 2'-FL within a physiologically relevant concentration range. The levels
288 of 2'-FL in urine have been shown to correspond to levels in the milk. Goehring et al. found the
289 urine of breast-fed babies of secretor mothers to contain 2'-FL in the range of 35-191 mg/L⁵⁵.
290 The assay responded to both low (20 mg/L) and high (200 mg/L) levels of 2'-FL spiked in urine
291 (**Figure 4C**). Importantly, we did not see any interference from the urine constituents with the
292 enzymes in our assay.

293

294 **Determination of fucosylation in glycoconjugates**

295 Glycoconjugates comprise a complex and diverse group of molecules that play important
296 biological roles. Current methods of analysis of these molecules also involve labor-intensive
297 procedures. We hypothesized that our paper-based scheme would be sufficient to analyze other
298 fucosylated glycoconjugates. We targeted the highly fucosylated blood group Lewis antigens,
299 specifically the Type 2 structures: composed of Gal- β (1,4)-GlcNAc, giving rise to Lewis^x (Le^x),
300 sialyl-Lewis^x (Sia-Le^x) and Lewis^y (Le^y). We also tested the blood group H antigen, which is the
301 fucosyl residue in blood group antigens. Due to the presence of either one or both of α -1,2/3/4-
302 linked fucose, we took a combinatorial approach. With antigen H type 2, a colorimetric change
303 was only observed with AfcA (**Figure 4D**). Similarly, Le^x was only detected in the presence of
304 AfcB. With Le^y antigen, a three-fold increase in signal in the presence of two fucosidases was
305 observed. Sia-Le^x is sialylated and we hypothesized that the sialic acid may interfere with the
306 fucosidase activity. To test the hypothesis, we also introduced an α -2,3-neuraminidase that can

307 cleave the sialic acid bound to the LacNAc. We observed a two-fold increase in the signal upon
308 removal of sialic acid. Although the assay is not orthogonal, it allows us to easily distinguish the
309 Lewis Type 2 antigens. This tool has the potential to determine the composition of HMOs in the
310 milk of mothers as determined by the Lewis blood group and hence, further aid in the
311 development of more personalized HMO supplementation. We next sought to determine if our
312 paper-based assay had the capacity to detect fucosylation in the context of more complex
313 biomolecules like glycoproteins. We targeted two common glycoproteins that are α -1,3-
314 fucosylated: horseradish peroxidase (HRP) and phospholipase A2 (PLA2) to serve as models.
315 Core α -1,3-Fuc is a common N-glycan modification found frequently on many plant and insect
316 glycoproteins, but not mammalian ones. Since this core antigen does not occur in mammals it
317 may be responsible for inducing immunogenic responses in mammals⁵⁶. These experiments
318 were consistent with our previous results; we were able to see a strong signal in the presence of
319 α -1,3 fucosidase with both glycoproteins (**Figure 4E**).

320 One common mammalian N-glycan modification is core α -1,6 fucosylation. To specifically
321 cleave α -1,6 fucosylated N-glycans, we produced AlfA from *Lactobacillus casei* by recombinant
322 expression in *E. coli* as described earlier. AlfA is an α -1,6 fucosidase, shown to have specific
323 hydrolytic activity on α -1,6 linked fucose⁵⁷. The recombinant enzyme was tested and validated
324 on 6'-fucosyl-GlcNAc and A1F-Glycan. 6'-Fuc-GlcNAc is an important modification of the core
325 glycan in N-glycoproteins. A1F-Glycan is a monosialo-fucosylated biantennary oligosaccharide,
326 found on different mammalian glycoproteins including IgG, gamma globulins, and many serum
327 glycoproteins. We observed a strong color change with both substrates and corresponded well
328 with the amount of fucose in the molecules (**Figure 4F**). The figures correspond to 0.4 μ g and 2
329 μ g of L-fucose in A1F-Glycan and 6'-Fuc-GlcNAc respectively. We also tested for the specificity
330 of AlfA: no signal was seen with α -1,2/3 linked fucosylated substrates (2'-FL and 3-FL
331 respectively). This indicates that the paper assay allows for efficient, linkage specific
332 quantification of fucosylation in N-glycans. We attempted to detect α -1,6 fucosylation in IgG

333 from human serum but did not see any signal, possibly due to fucose being below the limit of
334 detection. No color change was observed when we tried analyzing the isolated N-glycans by
335 treatment of IgG with endoglycosidase PNGase A/F.

336

337 **Discussion**

338 As the role of carbohydrate structures in myriad biological processes is increasingly recognized,
339 rapid and low-overhead analysis of carbohydrates becomes increasingly important. For
340 example, fucosylation in serum alpha-fetoprotein can serve as a marker for early diagnosis of
341 hepatocellular carcinoma⁵⁸. However, current methods of characterizing glycans, especially to
342 the level of linkage specificity, require expensive equipment and significant expertise. To enable
343 more practical methods of diagnosis or development of glycoprotein therapeutics, advances in
344 analytical glycomics are needed to overcome the bottlenecks associated with state-of-the art
345 technologies. Here we demonstrate a robust, inexpensive, high-throughput colorimetric assay
346 to quantify fucose in biologically relevant fucosylated molecules. The main advantage of this
347 assay is easy and quick way to perform it, enabling in-line detection of multiple samples in
348 parallel. This assay also minimizes the volume of sample needed for analysis. While this assay
349 can be useful in low-resource settings, it also has the potential to leverage the metabolic
350 engineering efforts for production of fucosylated glycans by enabling the high-throughput
351 screening of libraries of mutant variants. This can also provide a new approach for directed-
352 evolution efforts towards improved fucosyltransferase variants. In addition, integration of this
353 method with other glycosyl hydrolases beyond fucosidase could be leveraged to provide
354 comprehensive quantification of sugars and linkages in many complex carbohydrates. This
355 platform demonstrates high specificity, reproducibility and stability, which constitutes a
356 promising approach to be implemented as an easy-to-use protocol for sensitive and high-
357 throughput detection of fucose in biological samples.

358

359 **Acknowledgements**

360 This work was supported by Iowa State University Startup Funds. F.E. was funded by the NSF
361 Trinet Fellowship and Manley Hoppe Professorship. T.J.M. was partially supported by the
362 Karen and Denny Vaughn Faculty Fellowship. Frederick Robinson was supported by the NSF
363 BioMaP REU program. The authors thank Dr. Ludovico Cademartiri for assistance with wax-
364 printing. The authors also thank Dr. Lucas J. Showman at the W.M. Keck Metabolomics
365 Research Laboratory for helping to analyze the human breast milk samples.

366

367 **Competing Interests Statement**

368 The authors declare no competing interests.

369

370 **Online Methods**

371 **Chemicals and reagents**

372 All reagents used were of analytical grade. Tris-HCl buffer (pH 9.5) was used as the buffer
373 solution. 2-(p-iodophenyl)-3-(p-nitrophenyl)-5-phenyltetrazolium chloride (INT), phenazine
374 methosulfate (PMS), NADP⁺ and dimethyl sulfoxide (DMSO) were purchased from Sigma-
375 Aldrich (Millipore Sigma, St. Louis, MO). Luria-Bertani (LB) culture medium, kanamycin and
376 carbenicillin were obtained from Sigma-Aldrich. Isopropyl b-D-1-thiogalactopyranoside (IPTG)
377 was purchased from Invitrogen (Invitrogen, Carlsbad, CA). 2'-Fucosyllactose and 3-
378 fucosyllactose were a kind donation by Glycom (Glycom A/S, Denmark). L-fucose, GDP-fucose,
379 A1F-Glycan and 2-Acetamido-2-deoxy-6-O-(6-deoxy- α -L-galactopyranosyl)-D-glucopyranose
380 (Fuc- α -1,6-GlcNAc) were purchased from Carbosynth (Carbosynth, Berkshire, UK).
381 Phospholipase A2 (*Apis mellifera*) was purchased from Enzo (Enzo Life Sciences Inc.,
382 Farmingdale, NY) and horseradish peroxidase from Sigma. L-Fucose Assay Kit was purchased

383 from Megazyme. All assay reagents were stored at -20 °C. The assays were carried out at room
384 temperature.

385

386 **Bacterial strains and plasmids**

387 *E. coli* NEB 5-alpha (New England Biolabs Inc., Ipswich, MA) was used for routine cloning and
388 *E. coli* BL21 (DE3) was used for protein overexpression. Primers and synthetic DNA were
389 purchased from Integrated DNA Technologies (IDT). Construction of plasmid pAfcA and pAfcB
390 is reported in our previous work²⁸. Plasmids pAfcA and pAfcB comprises of a constitutive
391 promoter and the fucosidase gene cloned onto a G9m-2 vector. Plasmid pET28:FDH was
392 constructed by replacement of GFP in the pET28:GFP plasmid with the fucose dehydrogenase
393 (FDH) gene with a His-tag fusion at the N-terminal. The FDH gene was amplified by PCR from
394 the genomic DNA of *Bifidobacterium longum subsp. infantis* ATCC 15697™ (American Type
395 Culture Collection, Manassas, VA). The FDH fragment was assembled into the pET28b vector,
396 downstream of a T7 promoter, using NEBuilder® HiFi DNA Assembly Master Mix (New England
397 Biolabs Inc., Ipswich, MA). The AlfA gene from *L. casei* was constructed by DNA synthesis
398 (IDT) after codon-optimization for *E. coli* (IDT DNA Codon Optimization Tool). The gBlock was
399 amplified and assembled into the G9m-2 vector, downstream of the constitutive promoter.
400 Bacterial transformations were carried out using electroporation. The authenticity and
401 orientation of the inserts was confirmed by DNA sequencing at the Iowa State DNA Facility
402 (Ames, IA).

403

404 **Proof of concept using commercial kit**

405 To test for the viability of using INT/PMS for a colorimetric readout for assaying free fucose, we
406 used a L-Fucose Assay Kit (Megazyme Inc., Chicago, IL). Different concentrations of L-fucose
407 were prepared and the assay carried out in a 96-well plate, according to the protocol supplied
408 by the manufacturer. 2 µL of the dye mix was added to the reaction mixes and allowed to react

409 for 5 mins. To test for the release of fucose from 2'-FL and 3-FL, a range of concentrations of
410 the oligosaccharides were incubated with lysate from cells expressing pAfcA and pAfcB
411 respectively, and followed by the kit protocol. The absorbance at 500 nm was monitored
412 throughout the reaction.

413

414 **Enzyme isolation**

415 The fucosidase and FDH expressing strains were cultured in 50 mL of LB medium at 37 °C at
416 250 rpm, overnight with appropriate antibiotics (carbenicillin, 50 ug/ml and 30 ug/ml kanamycin,
417 respectively). The pET28:FDH was induced with IPTG (0.5 mM) at mid-log phase. These
418 cultures were then incubated at 37 °C in a rotary shaker (250 rpm) for 16 hr. The overnight
419 cultures were washed and resuspended in 2 mL water, and lysed by sonication (10 min, 30 s
420 pulse, 30 s off, 30% amplitude). Debris was removed from lysates by centrifugation at 5000 xg
421 for 30 mins and the supernatant stored at 4 °C. One unit of α -1,2-L-fucosidase activity was
422 defined as the amount of enzyme required to release one mmol of L-fucose per minute from 2'-
423 FL (2 mM) in sodium phosphate buffer (10 mM), pH 7 at 30 °C. The N-terminally His-tagged
424 FDH was purified from the lysate under native conditions using the QIAexpress Ni-NTA Fast
425 Start Kit (Qiagen, Valencia, CA). 5 μ l of each fraction was mixed with 5 μ l of 2x Laemmli
426 Sample Buffer (Bio-Rad, Hercules, CA). Each sample was heated at 95°C for 5 minutes and
427 resolved on SDS-PAGE. The gel was visualized by Coomassie brilliant blue staining. The
428 apparent molecular weight of FDH was approximately 32 kDa. The protein expression yields
429 were calculated using a NanoDrop One Spectrophotometer (Thermo Scientific, Waltham, MA).

430

431 **Fabrication of paper-based sensor**

432 The patterns for this study were printed on Whatman® grade 3 filter papers via wax-printing.
433 They were purchased as sheets measuring 460 mm x 570 mm and cut to letter-size. Filter
434 paper (Whatman #3) was chosen for its wicking properties and sturdiness, compared to filter

435 papers of other thicknesses. The detection zone patterns were designed as circles with 7mm
436 inner diameter and 1 mm thickness on Adobe Illustrator (Adobe, San Jose, CA). The detection
437 zones were printed with a Xerox Color Qube 8570DN™ (Xerox, Norwalk, CT) printer using
438 black hydrophobic wax-based ink.
439 The printed paper was placed in an oven set at 180 °C for 5 mins. To assess if the hydrophobic
440 barriers fully penetrated the paper, water was spotted onto the detection zones to identify any
441 bleeding and cross contamination between zones. If the water bled through, the paper was
442 reheated and tested again till no bleed through was observed. The paper was used once cooled
443 to room temperature. A layer of single-sided tape was used to seal the bottom side of the paper
444 to contain the liquid within the barrier and prevent leakage.

445

446 **Performing paper-based assay**

447 The lysates containing the enzymes were spotted at the center of the detection zones and
448 allowed to dry. A 20 µL reaction system contained 2.5 µM NADP⁺, 1.25 mM INT (in DMSO) and
449 0.5 mM PMS (in DMSO). Table 1 shows a full listing of volumes of reagents required per
450 reaction. A mastermix containing all the reagents excluding the enzymes and the dye was
451 made and added to each well. The reactions were initiated by addition of the
452 samples/standards, immediately followed by the addition of the dye reagent. Reactions were set
453 up under low-light conditions. A color change was observed within 5 mins. All measurements
454 were performed in triplicate. The paper was left to incubate in the dark till dry. Once dry, the
455 paper was scanned using an Epson Perfection V800 Photo Scanner. To evaluate the limit of
456 detection and generate a standard curve, a series of dilutions of 2'-FL/3-FL were made and
457 analyzed. Data were fit via non-linear regression analysis using MATLAB.

458

459 **Image and Statistical Analysis**

460 The scanned images were analyzed on ImageJ that provided intensity data for each reaction.
461 The MicroArray plugin was used that uses internally controlled regions of interest (ROI) and can
462 measure microarray image stacks. The RGB channels were split and intensities were analyzed
463 in the green channel and the mean values recorded. The background from the control with no
464 analyte was calculated for each measurement. Calibration curves (**Figure 3C, 3D**) were built to
465 get a quantitative readout from the measured transmittance. Comparison of our assay against a
466 commercial microplate-reader was also carried out. We defined the LoD as the lowest fucose
467 concentration that gave a colorimetric signal significantly above the control (no fucosylated
468 analyte) sample ($P \leq 0.01$). P values were determined by performing a paired parametric t test
469 on Origin. To compare the analytical performance of our assay on biological fluids, we analyzed
470 6 random trials, with one half of the experimental data set allocated toward blind testing.

471 **Table 1: Procedure for running assay**

Reagent	Standard	Blank	Sample
Distilled water	10 μ L	11 μ L	10 μ L
Buffer	2 μ L	2 μ L	2 μ L
NADP ⁺	0.5 μ L	0.5 μ L	0.5 μ L
FDH	0.1 μ L	0.1 μ L	0.1 μ L
Fucosidase	1 μ L	1 μ L	1 μ L

Sample/standard	5 μ L	-	5 μ L
INT/PMS dye	2 μ L	2 μ L	2 μ L

472

473

474 **Long term stability of the paper-based assay**

475 To assess the stability of the paper assay, the AfcA enzyme lysates were spotted onto the
476 detection zones and left to air-dry in the fume hood for an hour at room temperature. Another
477 batch of spotted paper was subjected to lyophilization overnight. The papers were either stored
478 at room temperature or at 4 °C in plastic bags with silica pouches in the dark. To determine the
479 enzymatic activity after specific storage time, the assays for detection of 2'-FL were carried out
480 over a period of 45 days by rehydration with standard solutions. The colorimetric output was
481 analyzed as described earlier. All measurements were carried out at room temperature and in
482 triplicates.

483

484 **Analysis of biological samples**

485 Pooled, deidentified human breast milk samples were purchased from BioIVT (Westbury, NY).
486 Surine™ Negative Urine Control was purchased from Cerilliant (Cerilliant Co., Round Rock,
487 TX). HMOs were extracted from human breast milk using established procedures. 200 μ L of
488 milk was centrifuged at 9,000 rpm for 20 mins at 4 °C to remove lipids. After the top layer was
489 removed, 400 μ L of ethanol was added and centrifuged at 9,000 rpm for 10 mins at 4 °C and
490 the supernatant collected. The ethanol was removed by vacuum centrifuging and reconstituted
491 in water to different concentrations before analysis using the assay and validation of relative
492 abundance carried out using LC-MS/MS. We used an Agilent Technologies 1100 Series HPLC
493 system coupled to an Agilent Technologies Mass Selective Trap SL detector (Agilent

494 Technologies, Santa Clara, CA) equipped with an electrospray ion source (ESI) and controlled
495 by ChemStation A.10.02, including data acquisition and processing. Both MS and MS/MS
496 spectra were acquired in the negative-ion mode with an acquisition rate of 1 s per spectrum
497 over ranges of m/z 300 to 2,000 (for MS) and m/z 50 to 2,000 (for MS/MS). Precursor-ion
498 selection was performed automatically by the data system based on ion abundance. Three
499 precursors were selected from each MS spectrum to carry out product-ion scanning. Products
500 were analyzed on a Prevail Carbohydrate ES (250 mm × 4.6 mm id; 5 μm; Alltech Associates,
501 Deerfield, IL). The mobile phase consisted of water (aqueous solution containing 5 mM
502 ammonium acetate) and acetonitrile (AcN containing 5 mM ammonium acetate). The solvent
503 gradient was delivered at a flow rate of 1 ml/min and consisted of an initial linear increase from
504 85% to 50% AcN over 10 min, held at 50% AcN for 2 mins and followed by a linear decrease to
505 starting conditions for 2 min. The injection volume was 5 μl. The dynamic range and linearity
506 for the quantification of 2'-FL and 3-FL were evaluated through the use of a series of dilutions as
507 standard curves. To analyze 3-FL, the samples were concentrated in a vacuum centrifuge
508 (Eppendorf, Hauppauge, NY). Disparities with other cited literature may be due to different
509 analytical technique and differences in biochemical extraction process.

510 References

- 511 1. Dalziel, M., Crispin, M., Scanlan, C. N., Zitzmann, N. & Dwek, R. A. Emerging principles for
512 the therapeutic exploitation of glycosylation. *Science* **343**, 1235681 (2014).
- 513 2. Schneider, M., Al-Shareffi, E. & Haltiwanger, R. S. Biological functions of fucose in
514 mammals. *Glycobiology* **27**, 601–618 (2017).
- 515 3. Werz, D. B. *et al.* Exploring the structural diversity of mammalian carbohydrates
516 ('glycospace') by statistical databank analysis. *ACS Chem. Biol.* **2**, 685–691 (2007).
- 517 4. Lowe, J. B. The blood group-specific human glycosyltransferases. *Baillieres. Clin.*
518 *Haematol.* **6**, 465–492 (1993).

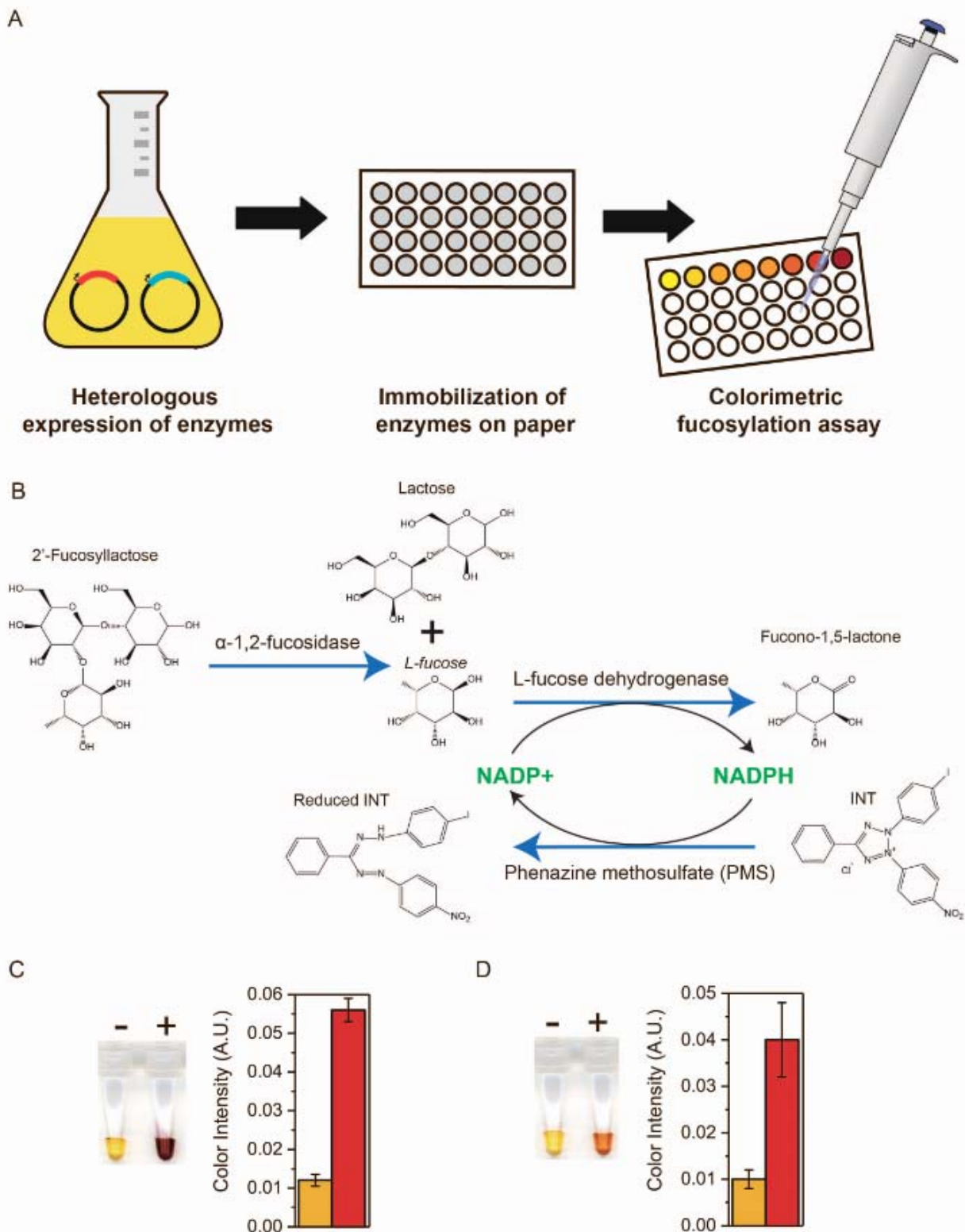
- 519 5. Ninonuevo, M. R. *et al.* A strategy for annotating the human milk glycome. *J. Agric. Food*
520 *Chem.* **54**, 7471–7480 (2006).
- 521 6. Stahl, B. *et al.* Oligosaccharides from Human Milk as Revealed by Matrix-Assisted Laser
522 Desorption/Ionization Mass Spectrometry. *Anal. Biochem.* **223**, 218–226 (1994).
- 523 7. Triantis, V., Bode, L. & van Neerven, R. J. J. Immunological Effects of Human Milk
524 Oligosaccharides. *Front Pediatr* **6**, 190 (2018).
- 525 8. Newburg, D. S. Oligosaccharides in human milk and bacterial colonization. *J. Pediatr.*
526 *Gastroenterol. Nutr.* **30 Suppl 2**, S8–17 (2000).
- 527 9. Bode, L. Human milk oligosaccharides: every baby needs a sugar mama. *Glycobiology* **22**,
528 1147–1162 (2012).
- 529 10. Yu, Z.-T. *et al.* The principal fucosylated oligosaccharides of human milk exhibit prebiotic
530 properties on cultured infant microbiota. *Glycobiology* **23**, 169 (2013).
- 531 11. Chichlowski, M., German, J. B., Lebrilla, C. B. & Mills, D. A. The influence of milk
532 oligosaccharides on microbiota of infants: opportunities for formulas. *Annu. Rev. Food Sci.*
533 *Technol.* **2**, 331–351 (2011).
- 534 12. Morrow, A. L., Ruiz-Palacios, G. M., Jiang, X. & Newburg, D. S. Human-milk glycans that
535 inhibit pathogen binding protect breast-feeding infants against infectious diarrhea. *J. Nutr.*
536 **135**, 1304–1307 (2005).
- 537 13. Newburg, D. S. *et al.* Innate protection conferred by fucosylated oligosaccharides of human
538 milk against diarrhea in breastfed infants. *Glycobiology* **14**, 253–263 (2004).
- 539 14. Goehring, K. C. *et al.* Similar to Those Who Are Breastfed, Infants Fed a Formula
540 Containing 2'-Fucosyllactose Have Lower Inflammatory Cytokines in a Randomized
541 Controlled Trial. *J. Nutr.* **146**, 2559–2566 (2016).
- 542 15. Appelmek, B. J. *et al.* Potential role of molecular mimicry between *Helicobacter pylori*
543 lipopolysaccharide and host Lewis blood group antigens in autoimmunity. *Infect. Immun.*
544 **64**, 2031–2040 (1996).

- 545 16. Appelmelk, B. J. & Vandenbroucke-Grauls, C. M. H pylori and Lewis antigens. *Gut* **47**, 10–
546 11 (2000).
- 547 17. Miyoshi, E. *et al.* Fucosylation is a promising target for cancer diagnosis and therapy.
548 *Biomolecules* **2**, 34–45 (2012).
- 549 18. Satoh, M., Iida, S. & Shitara, K. Non-fucosylated therapeutic antibodies as next-generation
550 therapeutic antibodies. *Expert Opin. Biol. Ther.* **6**, 1161–1173 (2006).
- 551 19. Raju, T. S. Terminal sugars of Fc glycans influence antibody effector functions of IgGs.
552 *Curr. Opin. Immunol.* **20**, 471–478 (2008).
- 553 20. Kandzia, S. & Costa, J. N-glycosylation analysis by HPAEC-PAD and mass spectrometry.
554 *Methods Mol. Biol.* **1049**, 301–312 (2013).
- 555 21. Grass, J. *et al.* Discovery and structural characterization of fucosylated oligomannosidic N-
556 glycans in mushrooms. *J. Biol. Chem.* **286**, 5977–5984 (2011).
- 557 22. Tsay, G. C. & Dawson, G. A sensitive spectrophotometric method for detection of l-fucose.
558 *Anal. Biochem.* **78**, 423–427 (1977).
- 559 23. Seydametova, E. *et al.* Development of a quantitative assay for 2'-fucosyllactose via one-
560 pot reaction with α 1,2-fucosidase and l-fucose dehydrogenase. *Anal. Biochem.* **582**,
561 113358 (2019).
- 562 24. Seydametova, E., Shin, J., Yu, J. & Kweon, D.-H. A Simple Enzymatic Method for
563 Quantitation of 2'-Fucosyllactose. *J. Microbiol. Biotechnol.* **28**, 1141–1146 (2018).
- 564 25. van der Meer, J. R. & Belkin, S. Where microbiology meets microengineering: design and
565 applications of reporter bacteria. *Nat. Rev. Microbiol.* **8**, 511–522 (2010).
- 566 26. Harms, H., Wells, M. C. & van der Meer, J. R. Whole-cell living biosensors--are they ready
567 for environmental application? *Appl. Microbiol. Biotechnol.* **70**, 273–280 (2006).
- 568 27. Sylvia Daunert, *. *et al.* Genetically Engineered Whole-Cell Sensing Systems: Coupling
569 Biological Recognition with Reporter Genes. *Chem. Rev.* **100**, 2705–2738 (2000).
- 570 28. Enam, F. & Mansell, T. J. Linkage-Specific Detection and Metabolism of Human Milk

- 571 Oligosaccharides in *Escherichia coli*. *Cell Chem Biol* **25**, 1292–1303.e4 (2018).
- 572 29. Martinez, A. W., Phillips, S. T., Whitesides, G. M. & Carrilho, E. Diagnostics for the
573 developing world: microfluidic paper-based analytical devices. *Anal. Chem.* **82**, 3–10
574 (2010).
- 575 30. Vella, S. J. *et al.* Measuring markers of liver function using a micropatterned paper device
576 designed for blood from a fingerstick. *Anal. Chem.* **84**, 2883–2891 (2012).
- 577 31. Hice, S. A., Santoscoy, M. C., Soupir, M. L. & Cademartiri, R. Distinguishing between
578 metabolically active and dormant bacteria on paper. *Appl. Microbiol. Biotechnol.* **102**, 367–
579 375 (2018).
- 580 32. Worramongkona, P. *et al.* A Simple Paper-based Colorimetric Device for Rapid and
581 Sensitive Urinary Oxalate Determinations. *Anal. Sci.* **34**, 103–108 (2018).
- 582 33. Asakuma, S. *et al.* Physiology of consumption of human milk oligosaccharides by infant
583 gut-associated bifidobacteria. *J. Biol. Chem.* **286**, 34583–34592 (2011).
- 584 34. Enam, F. & Mansell, T. J. Analysis of Fucosylated Human Milk Trisaccharides in
585 Biotechnological Context Using Genetically Encoded Biosensors. *J. Vis. Exp.* (2019).
586 doi:10.3791/59253
- 587 35. Enam, F. & Mansell, T. J. Linkage-Specific Detection and Metabolism of Human Milk
588 Oligosaccharides in *Escherichia coli*. *Cell Chemical Biology* (2018).
589 doi:10.1016/j.chembiol.2018.06.002
- 590 36. Katayama, T. *et al.* Molecular cloning and characterization of *Bifidobacterium bifidum* 1,2-
591 alpha-L-fucosidase (AfcA), a novel inverting glycosidase (glycoside hydrolase family 95). *J.*
592 *Bacteriol.* **186**, 4885–4893 (2004).
- 593 37. Iselt, M., Holtei, W. & Hilgard, P. The tetrazolium dye assay for rapid in vitro assessment of
594 cytotoxicity. *Arzneimittelforschung* **39**, 747–749 (1989).
- 595 38. Choi, H. S., Kim, J. W., Cha, Y.-N. & Kim, C. A quantitative nitroblue tetrazolium assay for
596 determining intracellular superoxide anion production in phagocytic cells. *J. Immunoassay*

- 597 *Immunochem.* **27**, 31–44 (2006).
- 598 39. Lim, H. H. & Buttery, J. E. Determination of ethanol in serum by an enzymatic PMS-INT
599 colorimetric method. *Clin. Chim. Acta* **75**, 9–12 (1977).
- 600 40. Yang, Y. *et al.* Paper-Based Microfluidic Devices: Emerging Themes and Applications.
601 *Anal. Chem.* **89**, 71–91 (2017).
- 602 41. Martinez, A. W., Phillips, S. T., Butte, M. J. & Whitesides, G. M. Patterned Paper as a
603 Platform for Inexpensive, Low-Volume, Portable Bioassays. *Angew. Chem. Int. Ed Engl.*
604 **119**, 1340–1342 (2007).
- 605 42. Samyn, P. Wetting and hydrophobic modification of cellulose surfaces for paper
606 applications. *J. Mater. Sci.* **48**, 6455–6498 (2013).
- 607 43. Carrilho, E., Phillips, S. T., Vella, S. J., Martinez, A. W. & Whitesides, G. M. Paper
608 microzone plates. *Anal. Chem.* **81**, 5990–5998 (2009).
- 609 44. Carrilho, E., Martinez, A. W. & Whitesides, G. M. Understanding wax printing: a simple
610 micropatterning process for paper-based microfluidics. *Anal. Chem.* **81**, 7091–7095 (2009).
- 611 45. Baumgärtner, F., Seitz, L., Sprenger, G. A. & Albermann, C. Construction of *Escherichia*
612 *coli* strains with chromosomally integrated expression cassettes for the synthesis of
613 2'-fucosyllactose. *Microb. Cell Fact.* **12**, 40 (2013).
- 614 46. Huang, D. *et al.* Metabolic engineering of *Escherichia coli* for the production of 2'-
615 fucosyllactose and 3-fucosyllactose through modular pathway enhancement. *Metab. Eng.*
616 **41**, 23–38 (2017).
- 617 47. Albermann, C., Piepersberg, W. & Wehmeier, U. F. Synthesis of the milk oligosaccharide
618 2'-fucosyllactose using recombinant bacterial enzymes. *Carbohydr. Res.* **334**, 97–103
619 (2001).
- 620 48. Erney, R. M. *et al.* Variability of human milk neutral oligosaccharides in a diverse
621 population. *J. Pediatr. Gastroenterol. Nutr.* **30**, 181–192 (2000).
- 622 49. McGuire, M. K. *et al.* What's normal? Oligosaccharide concentrations and profiles in milk

- 623 produced by healthy women vary geographically. *Am. J. Clin. Nutr.* **105**, 1086–1100 (2017).
- 624 50. Maltesen, M. J. & van de Weert, M. Drying methods for protein pharmaceuticals. *Drug*
625 *Discov. Today Technol.* **5**, e81–8 (2008).
- 626 51. Liao, Y.-H., Brown, M. B. & Martin, G. P. Investigation of the stabilisation of freeze-dried
627 lysozyme and the physical properties of the formulations. *Eur. J. Pharm. Biopharm.* **58**, 15–
628 24 (2004).
- 629 52. Totten, S. M. *et al.* Comprehensive profiles of human milk oligosaccharides yield highly
630 sensitive and specific markers for determining secretor status in lactating mothers. *J.*
631 *Proteome Res.* **11**, 6124–6133 (2012).
- 632 53. Pausan, M.-R., Kolovetsiou-Kreiner, V., Richter, G. L. & Madl, T. Human Milk
633 Oligosaccharides modulate the risk for preterm birth in a microbiome dependent and
634 independent manner. doi:10.1101/683714
- 635 54. Rudloff, S., Pohlentz, G., Borsch, C., Lentze, M. J. & Kunz, C. Urinary excretion of in vivo
636 ¹³C-labelled milk oligosaccharides in breastfed infants. *Br. J. Nutr.* **107**, 957–963 (2012).
- 637 55. Goehring, K. C., Kennedy, A. D., Prieto, P. A. & Buck, R. H. Direct evidence for the
638 presence of human milk oligosaccharides in the circulation of breastfed infants. *PLoS One*
639 **9**, e101692 (2014).
- 640 56. Prenner, C., Mach, L., Glössl, J. & März, L. The antigenicity of the carbohydrate moiety of
641 an insect glycoprotein, honey-bee (*Apis mellifera*) venom phospholipase A2. The role of
642 alpha 1,3-fucosylation of the asparagine-bound N-acetylglucosamine. *Biochem. J* **284 (Pt**
643 **2)**, 377–380 (1992).
- 644 57. Rodríguez-Díaz, J., Monedero, V. & Yebra, M. J. Utilization of natural fucosylated
645 oligosaccharides by three novel alpha-L-fucosidases from a probiotic *Lactobacillus casei*
646 strain. *Appl. Environ. Microbiol.* **77**, 703–705 (2011).
- 647 58. Gish, R. G. Early detection of hepatocellular carcinoma through surveillance using
648 biomarkers. *Gastroenterol. Hepatol.* **10**, 121–123 (2014).

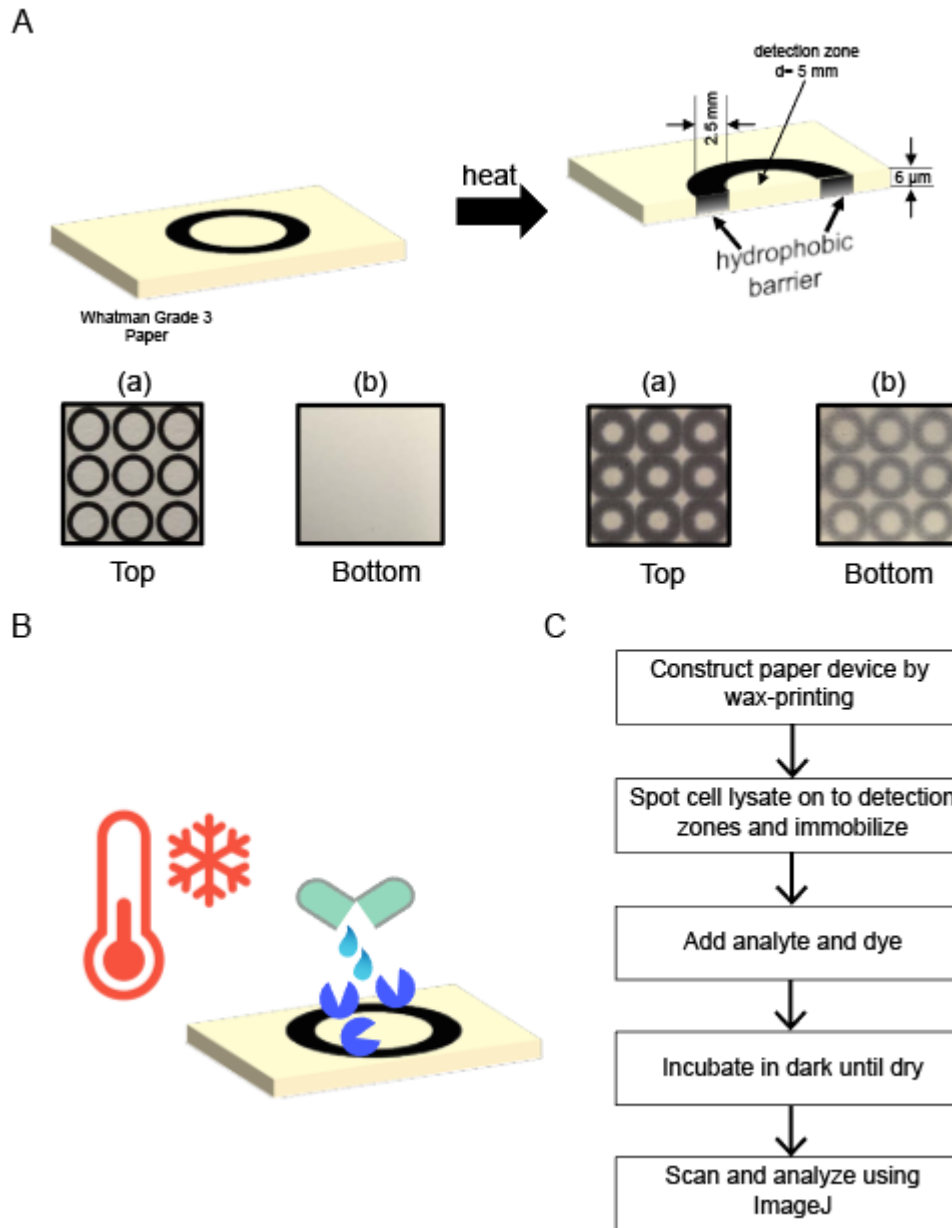


649

650 **Figure 1: Strategy for paper-based sensing of fucosylation. (A)** Schematic illustrating the

651 immobilization of the enzymes on to the paper device and development of colorimetric signal

652 upon addition of analyte. **(B)** Reaction mechanism for detection of fucose using a linkage
653 specific fucosidase coupled to a colorimetric assay based on INT tetrazolium dye, 2'-FL shown
654 here. **(C)** Images of reaction with free fucose (left) and 2'-FL (right) at 300 mg/L.

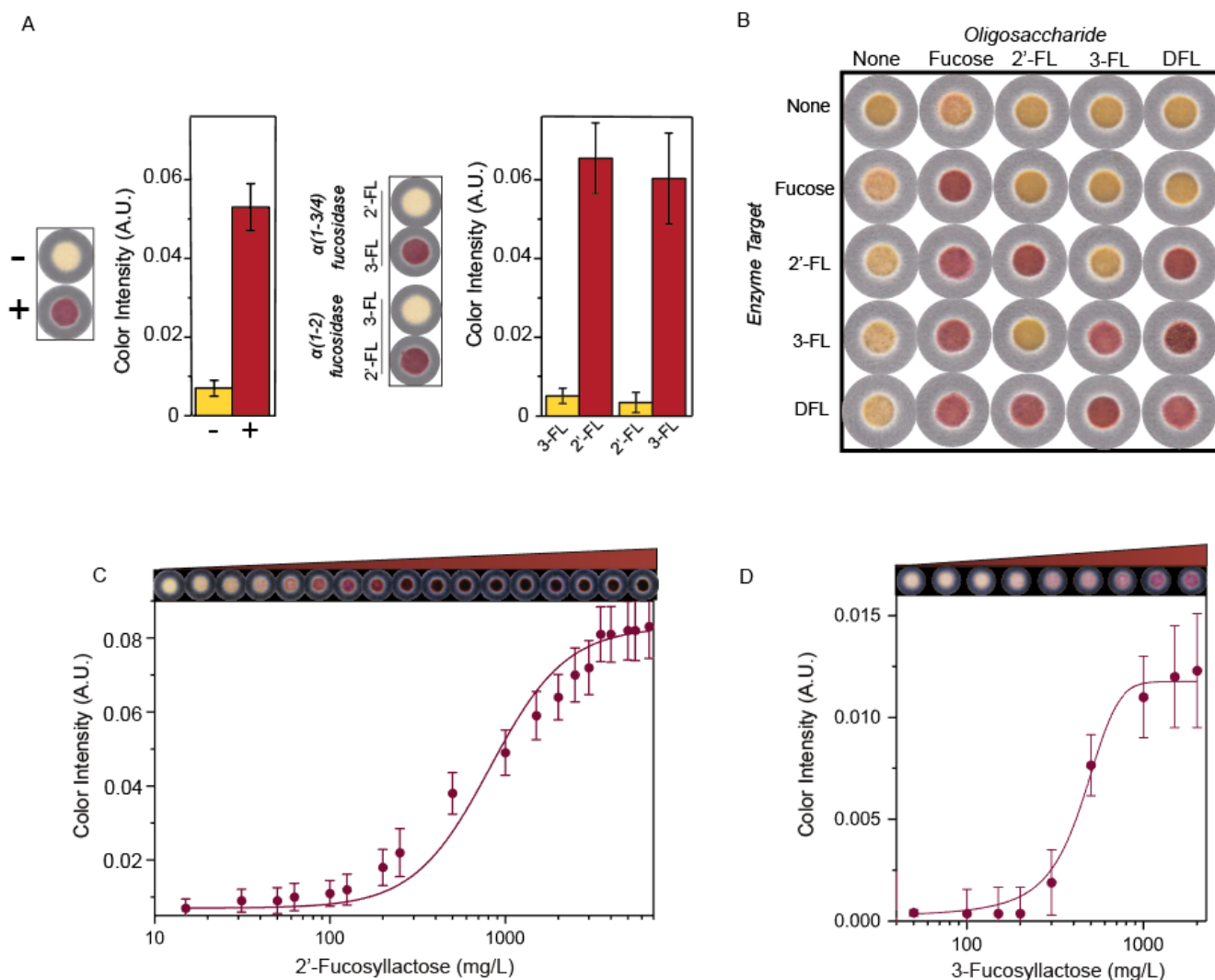


655

656 **Figure 2: Schematic describing the design and process of setting up the paper-based**

657 **assay.** **(A)** Layout of the wax printed array. Top panel shows the dimensions of the wells.

658 Bottom panel shows the printed array before and after heating, as seen on the top and bottom
 659 surface of the paper. **(B)** Cell lysate containing recombinantly expressed enzymes is spotted on
 660 the wells and immobilized. **(C)** Overview of the workflow of the assay.



661

662 **Figure 3: Determination of fucosylation in HMOs using paper device. (A)** Reaction

663 with free fucose (left) and fucosylated HMOs, 2'FL and 3-FL (right). Assays were

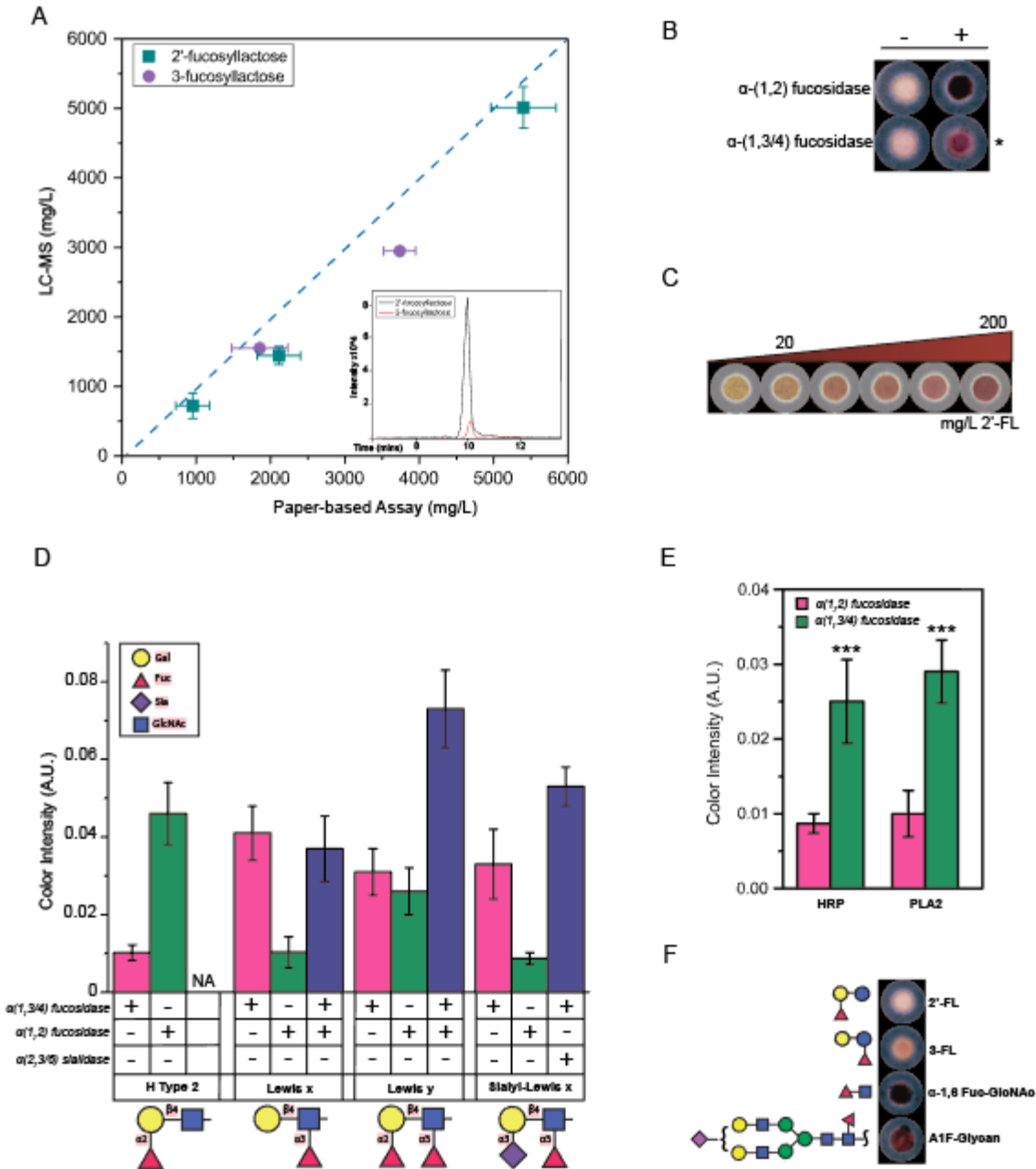
664 performed with 500 mg/L of L-fucose, 2'-FL and 3-FL **(B)** A 25-reaction array with two

665 different linkage specific fucosidases in different combinations. Image was captured after

666 the paper was dry. **(C)** Transfer function for sensing 2'-FL. Response curve depicts

667 mean color intensity (analyzed in triplicate). The dose-response curve was fitted with a
668 4PL model, shown by the line. The top shows a capture of the signal expression from
669 increasing concentrations of 2'-FL. **(D)** Calibration curve for 3-FL, as described in (C).
670 Error bars represent standard deviation of triplicate measurements of mean color
671 intensities.

672



673

674 **Figure 4: Paper-based assay enables determination of fucosylation type in biological**

675 **fluids and glycoconjugates. (A)** Comparing measurement of concentrations of 2'-FL and 3-FL

676 in human breast milk using paper-based assay and HPLC/MS. Lipids and proteins were

677 removed before analysis. To analyze 3-FL, samples were concentrated. Inset shows

678 chromatogram peaks for 2'-FL (black) and 3-FL (red). **(B)** Arrayed image showing colorimetric
679 output from assay on breast milk samples. * indicates concentrated samples tested. **(C)** Testing
680 for 2'-FL in spiked synthetic urine at levels found in maternal and infant urine. **(D)**
681 Distinguishing Lewis Type 2 antigens and quantification of their fucosylation. **(E)** α -1,3-
682 Fucosylation in glycoproteins. Differences in the means of the test conditions and the controls
683 were analyzed using a t-test (***P < 0.0001). **(F)** Determination of α -1,6-fucosylation in N-
684 glycans. 2'-FL and 3-FL were used as controls.